NASA

Technical Memorandum 83835

MATTER ACCRETING NEUTRON STARS

P. MÉSZÁROS

SEPTEMBER 1981

National Aeronautics and
Space Administration

Goddard Space Flight Center
Greenbelt, Maryland 20771

MATTER ACCRETING NEUTRON STARS†

P. Mészáros*
Laboratory for High Energy Astrophysics, Code 665
NASA/Goddard Space Flight Center, Greenbelt, MD 20771, U.S.A.

ABSTRACT: Some of the fundamental neutron star parameters, such as the mass and the magnetic field strength, have been experimentally determined in accreting neutron star systems. We review here some of the relevant data and the models used to derive useful information from them, concentrating mainly on X-ray pulsars. We then discuss the latest advances in our understanding of the radiation mechanisms and the transfer in the strongly magnetized polar cap regions.

I. INTRODUCTION

A significant fraction of the known celestial X-ray point sources have been recognized as neutron stars in close binary orbit around a normal star companion, while in a number of γ-ray burst events there are strong indications pointing to a neutron star origin, binary membership being as yet unclarified. With a few exceptions, we shall be dealing with those systems where the neutron star appears as an X- or γ-ray pulsar powered by mass infall. X-ray bursts, some of which are thought to be thermonuclear flashes on low-magnetic field neutron stars, are dealt with elsewhere in this volume (1). Unlike the rotation-powered radio pulsars, some of which also emit X-rays and γ-rays, the accretion-powered neutron stars, whether pulsing or not, emit their energy almost exclusively above the keV range. Among these systems, those that do show regular pulsations are the subject of the most vigorous inquiries, since they provide a particularly useful laboratory for testing our knowledge of nuclear and particle physics, as well as of general

*Also at the University of Maryland. On leave of absence from Max-Planck-Institut für Physik und Astrophysik MPA, Garching.

†Text of an invited review presented at the Symposium on Neutron Stars, 5th General Conference of the European Physical Society, Istanbul, Turkey, 1981.

relativistic stellar structure, binary evolution, strong magnetic field plasma physics and radiative transfer. Experimental determinations of the neutron star masses, magnetic field strengths, and indirectly radii, have become available, as well as spin periods and period decrements, orbital periods, pulse shapes and electromagnetic spectra above a few tenths of keV, all of which provide a powerful tool, as well as challenge, for theories and models.

While the standard interpretation of binary X-ray sources, wherein the gas lost from the visible companion is captured and heated to high temperatures by the neutron star (2,3,4), has, on the whole, proved remarkably satisfactory, there are a number of tantalizing ambiguities about most of the processes involved. In its simplest version, the model envisages the mass exchange occurring either by slow leakage (Roche lobe overflow) or by capture from a stellar wind from the companion. In the first case, the matter's angular momentum causes an accretion disk to form, or in the second case, its random value leads to a quasispherical inflow. This spiralling or quasiradial inflow is assumed to be stopped by the pressure of the neutron star's magnetic field at the Alfvén surface, unless if the field has decayed. The accreted matter is threaded by the field and is conveyed to the polar caps at ~ free fall velocity, where abrupt deceleration and heating occurs either by particle collisions, collective effects or radiation pressure. Pulsed emission is due to the spin of the neutron star and the anisotropic emitting pattern, or periodic occultation by matter at the Alfvén shell. We list below some of the relevant X-ray data and their interpretation, including some of the γ-ray burst information where it relates to neutron stars.

II. PULSE PERIODS AND MASS EXCHANGE MECHANISMS

The pulsation periods of upwards of 10 X-ray pulsars are known, typically to 6 figure accuracy, ranging from about 1 sec to about 10^3 sec (5). A strong clue for distinguishing between the two possible modes of mass exchange, has been found for those X-ray

pulsars where besides the period P also the period decrement $\dot{P}$ is known. Calculations of the torque exerted on the neutron star by an accretion disk interacting with the dipole field of the neutron star at the Alfvén radius (where $B^2/8\pi \sim \frac{1}{2}\rho v_\phi^2$) give a well defined theoretical relationship between the period change $-\dot{P}$ and the quantity $(PL^{3/7})$, L being the luminosity (6,7). The observations available for 10 pulsars give a fairly good agreement with this relationship utilizing a magnetic field typical of neutron stars (see Figure 1). A comparable theoretical relationship for the wind transfer case, on the other hand, is not readily available, estimates (7) suggesting the absence of a fit. This is partly due to insufficient development of the wind theory in an aspherical potential, where the atmosphere may also be disturbed by X-rays from the companion. The interaction of the wind, and alas also of the disk, with the magnetic field is made difficult due to uncertainties concerning conductivity, turbulence and viscosity, e.g., (8, 9) for reviews. On the face of it, it would seem that binary X-ray pulsars tend to appear in systems with accretion disks. On the other hand, there is evidence for wind transfer in a number of X-ray binaries (10) including some X-ray pulsars (e.g., 4U0900-40 ≡ Vela X-1). This seems consistent with the fact that this object falls outside the "disk" relationship of Figure 1. In another case (Cen X-3), there is evidence for a wind, but it has been argued that a disk would nonetheless form (11), although this is not the case for most wind sources. Other neutron stars may exist in disk systems where pulsations are not detected because of the beam not intersecting the observer, or in wind cases, because of scattering on the surrounding flow. Interestingly, in the γ-ray burst of March 5, 1979, where the energy source is unlikely to be accretion but it is also believed to be a neutron star (12), an 8-second period has been detected (13).

III. PULSE SHAPES AND PULSATIONS MECHANISMS

A large body of information exists about the pulse shapes of X-ray pulsars (see Figure 2) which contain information on the nature of the mechanism for producing pulsations. The pulse shapes range

from being strongly dependent on energy (e.g., Her X-1) to showing very little change with energy (e.g., Cen X-3). The multiplicity of the pulse structure is often also a function of energy, and the duty cycles are invariably large ($\lesssim$ .5). Both symmetric, and highly assymmetric pulse shapes appear in different objects. There are two principal mechanisms for producing pulses, one of them relying on the intrinsic beaming of the radiation pattern, caused by anisotropies in the radiative transfer or the accretion flow, and the other relying on periodic occultation of the emitting surface by an opaque screen near the Alfvén surface, revolving at the pulse frequency. In the first one, an energy dependent pulse profile is expected, the cross sections in the strong field of the polar caps being frequency and angle dependent, while in the second, only in the photoabsorption range 1-6 keV is a dependence expected, the opacity at the Alfvén surface above 6 keV being essentially Thomson. In the case of Her X-1, the observation of a soft X-ray flux (14) in antiphase with the hard X-ray pulses can be readily interpreted as being due to the hard X-rays being absorbed in the screen (15,16,17) followed by reemission at lower frequencies. Photo absorption in the range $1 < h\nu < 6$ keV would explain the sharp pulse edges, but would also predict stronger modulation in this range than at higher energies, which is not observed (17). On the other hand, recently some detailed calculations of intrinsic beam patterns from homogeneous magnetized atmospheres have been made (18,19), which indicate that the duty cycle, energy dependence and multiplicity of pulses can be reproduced, but difficulties remain in explaining the steep edges and the asymmetry of some pulses. The observation of a hardening of the spectrum towards the middle of the pulse (20), and the apparent trend shown by e.g., Her X-1, A0535+26 and 4U0900-40 of the simple pulse structure breaking up into multiple pulses as increasingly lower energies are sampled has also been found in intrinsic beam calculations (18). Neither the intrinsic beam nor the opaque shell models are self-consistent as yet. In the first, the atmosphere structure (gradients) remains to be elucidated, in the second, the dynamics and the geometry of the opaque shell is uncertain. A very valuable observation would be to determine the

polarization of the pulses as function of phase, since the predicted intrinsic polarization (18) is much greater than for the shell case (17) at low energies.

IV. SPECTRUM

There is also much information on the spectra of X-ray pulsars, most objects having a rather flat power law energy index between a few keV to several tens of keV, and dropping abruptly above that (e.g., 21,22,23). Line features ascribed to Fe are sometimes present in the 6-8 keV region (24,25,26). Other lines, ascribed to the cyclotron process, will be discussed in Section VI. The Fe lines, having widths of a few keV, may originate near the Alfvén surface (27,28), since they are rather narrow. The continuum, on the other hand, must originate near the surface, to explain the large luminosities, often near the Eddington value. As an example, the spectrum of Her X-1 is shown in Figure 3. While naively the power law photon spectra resemble somewhat an optically thin bremsstrahlung, the actual situation, even for a homogeneous atmosphere is more complex. The polarization structure of the magnetized medium introduces a subtle interplay whereby photons are created in one polarization and escape in the other (29,30), the thermalization length being a function of frequency. A simple homogeneous atmosphere, if only bremsstrahlung and coherent scattering is assumed, will look like optically thin bremsstrahlung only when very low optical depths are assumed, which do not produce the required luminosity for a galactic X-ray source. Increasing the optical depth increases the luminosity, but the two-polarization coherently scattered spectrum then turns over at low frequencies too early. The inclusion of comptonization (incoherent scattering) may be the answer, although existing Monte Carlo calculations (31,32,33) with this effect included still turn over too early. Analytic and numeric integration of the incoherently scattering transfer equations (34,35) suggests, however, that one may reproduce a power law down to low frequencies.

V. MASS DETERMINATIONS

This is a crucial parameter from the evolutionary and microphysical point of view, which we review here only briefly. A number of neutron star masses have been determined using the dynamical laws governing the orbital motion in the binary system. The simplest case is that when one has i) the doppler delay curve for the pulses from the neutron star, ii) the doppler delay curve for the companion (e.g., its absorption line frequencies), iii) an eclipse of the neutron star by the companion. i) yields $a_x \sin i$, the projection of the NS orbit's semimajor axis, giving the mass function $f(M_x, M_v, i) = 4\pi^2(a_x \sin i)^3/G\, P^2_{orb} = M_v \sin^3 i/(1+q)^2$, where $q \equiv M_x/M_v$, $i \equiv$ angle between the planes of the sky and the orbit. ii) yields $a_v \sin i$ of the visual orbit, and $q = a_v \sin i / a_x \sin i = K_v P_{orb} (1-e^2)^{1/2}/2\pi a_x \sin i$, $K_v \equiv$ semiamplitude of the visual doppler velocity curve, $e \equiv$ eccentricity. iii) yields θ_e, the eclipse half angle, linked to the stellar and Roche radii R_* and R_L by $R_* = D\,(\cos^2 i + \sin^2 i \sin^2 \theta_e)^{1/2} = \beta D(a-b \log q)$, where D = separation, a,b = constants depending on the ratio $\Omega = \omega_{spin}/\omega_{orb}$, β = fraction of R_L filled out by R_*. Theoretical guesses at β and Ω lead then to a determination of M_x, i and e. Both the observational errors in $a_x \sin i$, K_v and θ_e, and the guesses of Ω, β lead to fairly large error bars. Values of M_x are plotted in Figure 4, where results for 5 X-ray pulsars, as well as that of the binary radio pulsar are plotted. For more details, see (36,5). The remarkable thing is that, within these 1σ error bars, they all agree with the range of masses (hatched area) expected on the basis of conventional nuclear and particle many-body physics.

Related to mass determinations are also a number of observations of a line feature at 400-460 keV in γ-ray burst sources (37,38,39), interpreted as 511 keV e^+e^- annihilation, redshifted by the gravitational field of a neutron star. While the energy source need not be accretion, the redshift values provide information on the ratio M/R which are in agreement with expected values for neutron stars. This is true also of the March 5, 1979 burst (12), which showed pulsations indicative of being a neutron star (13). Calculations of annihilation spectra (40,41) indicate that the

"line" frequency shifts to the blue with increasing temperature, above a few x 10^8 ^{o} K, so the interpretation of the line frequency is not just given by gravitational redshift but the physics of the line formation as well.

VI. MAGNETIC FIELD STRENGTH

This is the area where most of the excitement has been lately. While initially researchers had to rely upon flux-freezing arguments, and use polarization measurements and theoretical considerations in radio pulsars to conclude that B ~ 10^{12}G, a ground breaking direct experimental determination of the magnetic field strength of the X-ray pulsar Her X-1 came forth in 1977 (42,43). A high altitude balloon experiment with a scintillation detector yielded a well defined line around 54 keV, with 15 σ significance, which could only be interpreted as a cyclotron line in a field of B = 4.4 10^{12} G, or 3.5 10^{12} G if in absorption (see Figure 3). This line was seen in three different flights by the original group, in one of the flights some evidence for a second harmonic being present (43), which however subsequently was not seen again, although this is consistent with the changes of the overall continuum between observations. While consistent results from other groups using similar resolution ($\lesssim$ 25 percent) (44,45) have been reported, a high resolution ($\lesssim$ 3 percent) Germanium experiment (46) came up with a feature at either 44 keV (emission) or 35 keV (absorption), and a line and continuum intensity which was within a factor 2 of previous values. Clearly further high resolution and high sensitivity measurements would be desirable to establish whether the line energy and intensity is a function of time, and perhaps of phase (e.g., (45)). Another X-ray pulsar for which a line feature has been reported is 4U0115+63 (47), and more recently, about thirty γ-ray burst sources have been found to show well defined line features in the range 40-60 keV (39). Implied field values would be in the range 2 10^{12} $\lesssim$ B $\lesssim$ 5 10^{12} G. While theoretically there is no difficulty in understanding qualitatively the production of cyclotron line features in steadily accreting

X-ray pulsar atmospheres (see below), the situation is less clear in the γ-ray burst sources, where relativistic temperatures exist at least initially, whereas the line widths suggest a lower temperature.

VII. PHYSICS OF THE STRONGLY MAGNETIZED ATMOSPHERE

On the theoretical side, this is the field which is most active at present. While nonmagnetic accreting neutron star atmospheres had been considered in (48,49,50), early work on magnetized atmospheres (51,52) had pointed out several interesting possibilities, such as cyclotron line features and intrinsic beaming. It was not however until the experimental detection of a cyclotron feature in Her X-1 (42,43) that work on the subject began on a wide scale. Early attempts at interpretation (53,54,55,56) drove home the fact that progress could only be made after a number of basic questions on the elementary proceses were cleared up.

The radiative cross sections were known to be strongly angle and frequency dependent in a magnetic field (57,58). Useful expressions were worked out in (60,61,62), elucidating the role of the ellipticity parameter and the normal polarization modes. Meanwhile, it had been pointed out that the vacuum polarization due to the virtual pairs in a strong magnetic field would influence polarization measurements (62). It was then realized that the vacuum polarization would also dominate the radiative cross sections and influence the spectrum, because of their dependence on the polarization normal modes (63,64,65). This effect can be thought of as being due to coherent forward scattering by virtual pairs, which for real densities $n_e \lesssim 10^{24}$ cm^{-3} and $B \gtrsim 10^{12}$ G is more important than scattering off the real electrons. While in a cold e^- plasma, which rotates right handed if looked along $\vec{B}$, only the right handed normal mode resonates at the cyclotron frequency, in the virtual e^+e^- plasma the right and left modes both resonate. This has also the effect of driving the usually elliptic modes towards being quasi linear. The large effect of the vacuum on the refractive index, and therefore on the polarization eigen-

modes $\vec{e}^{\,i}(\omega,\theta)$ of the plasma, has an equally large impact on all the radiative cross sections, because these are expressions of the form $d\sigma = \langle \vec{e}' | 0 | \vec{e} \rangle$. The angle and frequency dependence of the Compton, bremsstrahlung and cyclotron processes are strongly affected. Also, a second resonance feature appears at the frequency $\omega_o = 3(4 \times 10^{12} G/B)(n_e/10^{22} cm^{-3})^{1/2}$ keV, where the real and virtual particles cancel their effects mutually (66,67). It also became apparent that "real" cyclotron absorption, where a photon disappears, its energy going into thermal motion, would not be important since radiative deexcitations would far exceed collisional ones at the resonance. The dominant process at ω_H is just resonant scattering (29,30). Collision of electrons with thermal protons (bremsstrahlung) would be the photon production mechanism, expressions being given in (29), based on (68).

Using these cross sections, radiative transfer calculations were performed for uniform atmospheres, in the diffusion and two-stream approximations (29,30,66), including the frequency and polarization dependence of the cold plasma cross sections. These calculations revealed the importance of the mode exchange scattering $\sigma_{i \to j}$, which plays a crucial role in producing the cyclotron line (which would be absent if σ_{ij}, σ_{ji} were neglected). Photons are preferentially created in one mode, and escape in the other, depending on frequency. Incoherent scattering neglecting polarization effects was treated in (34) and in Monte Carlo calculations which also included thermal effects (31,32). Under coherent scattering, the cyclotron feature can appear either in emission or absorption, depending on whether a cooler spectrum is shined through a hotter gas or vice-versa (30). The inclusion of thermal and vacuum effects (69) can produce emission line profiles not unlike those observed in Her X-1, but this does not settle the emission versus absorption issue, until a self-consistent temperature structure for the atmosphere is known. The inclusion of quantum recoil effects in the cross sections and an analysis of the redistribution function for one (resonant) polarization (70) raised the possibility of the line being asymmetrical respect to the rest resonance frequency. Thermal and quantum recoil effects were self-

consistently included in (35), where the effect of incoherent scattering inside and outside the resonance was investigated by means of a two-angle multifrequency Feautrier scheme. Incoherent scattering may explain the continuation of a power law continuum down to the ~ 1 keV range, but the photon input source function is a function of the still unsolved temperature and density structure of the atmosphere.

The Coulomb collision of protons and electrons in a strong field had been investigated by (71,72,73) and, aside from possible collective effects (e.g., shock heating) this is the main candidate for a heating agent. Also, especially at low luminosities, where radiation pressure is negligible, and if a collionless shock does not arise, the stopping length of the infalling protons is a measure of the effective depth of the emitting atmosphere. The proton-electron binary collision cross section has been reevaluated in (74), where the effect of ion sound turbulence in the background plasma was considered, in (75), where knock-on collisions were also investigated, and in (76), where the e-e cross section was also evaluated. Except for (74), these results indicate longer stopping lengths than in the nonmagnetic case by a factor $1/\sin^2\theta$, where θ is proton pitch angle, due to the fact that the electrons can only take up longitudinal momentum. Incoming fast protons at $\theta \sim 0^\circ$ pitch angle would in this case be stopped rather by nuclear p-p collisions, $\ell_{pp} \sim 50$ g/cm^2. On the other hand, in (77,78) it is argued that, because the proton gyroradius is smaller than the Debye length of the plasma, the Coulomb stopping is more efficient than previously thought, values of $\ell_H \sim 5$-20 g/cm^2 being put forward. The cross sections (75,76) were also used in investigating the electron distribution function (79), finding some evidence for departure from a Maxwellian. These studies of the electron heating rate, together with previously mentioned ones on the radiative transfer, should be combined to obtain a self-consistent structure for the X-ray atmosphere, necessary both for calculating a realistic spectrum, and a realistic beaming pattern.

Intrinsic beaming patterns have until now been calculated for guessed atmosphere parameters. Monte Carlo calculations for an optically thin cyclinder illuminated from below were done in (80) and (33), which suggest a harder spectrum towards the equator. A plane parallel semi-infinite pure scattering atmosphere, with B perpendicular to the surface, was solved approximately in (81). This geometry leads to a pencil beam and can produce multiple pulses. The effect of absorption as well as scattering and polarization on the directionality was considered in (18,19, 82,83). In (19) the self-emission of a cylinder and a slab was solved by a Feautrier differential scheme, while in (18) the slab with background illumination and semi-infinite media with B perpendicular to the surface were solved with an integral scheme. Columns (fan beams) produce wider peaks than slabs (pencil beams) (19), and double peaks with a central hollow appear in pencil beams (18,19) as well as triple peaks and a hardening of the spectrum towards midpulse (18). These pulses appear to reproduce most of the major features of observed ones except the asymmetry and steep edges. To achieve this, it may be necessary to extend these calculations to distorted or non-dipole field configurations, although additional modulation by the Alfvén surface sould also help. An intrinsic component seems however necessary to explain the multiple peak structure, the energy dependence of the pulse width and the phase dependence of the spectrum.

The structure of the emitting atmosphere is largely still unknown. In the high luminosity pulsars, where the radiation pressure is sufficient to create a radiation-mediated shock, or deceleration zone, that stands off some distance d_s, a "pill-box" shaped atmosphere would arise at the base of the accretion column. Radiation would escape sideways (fan-beam) as well as perhaps upwards (85). The intriguing possibility also exists that, even in low luminosity pulsars, collisionless shocks may create a similar structure, but the plasma physics of such shocks is as yet unexplored in this context. Inhomogeneities may well arise due to instabilities (86). If shocks do not arise, the low luminosity pulsar atmospheres probably do not stick out significantly, the

energetic ($\frac{1}{2} m_p v_{ff}^2$) proton beam being decelerated by particle collisions in the denser part of the atmosphere. In this case, radiation escapes mostly upwards, producing a pencil beam (52). A self-consistent atmosphere structure calculation has been done approximately only for the shock models (85,87). It would be very important to verify whether shocks, radiative or otherwise, indeed occur, and some simple tests may be possible. If the sides do not emit at the blackbody limit ($\langle\omega\rangle < \omega_H$) the shock height $d_s \sim V t_c$, where V is post shock velocity and t_c is the Coulomb time for electron heating by the thermalized protons, so $d_s \sim n_e^{-1} \sim \dot{M}^{-1} \sim L^{-1}$. If the cyclotron line arises near the shock, one would expect a change of $\omega_H \sim (R_{NS} + d_s)^{-3} \sim (1 + \text{const} \times L^{-1})^{-3}$. Similarly, the pulses, if produced by the fan beam, would become broader as L goes down, because the surface curvature sampled increases with d_s, $\Delta\phi_{pulse} \sim d_s^{3/2} d_s^{-1} \sim d_s^{1/2} \sim L^{-1/2}$. If no shock arises, and one has an almost level hot spot producing a pencil beam, no such dependence of ω_H or $\Delta\phi$ on L would be expected, but a correlation should exist between the pulse multiplicity and the quantity ω_H/ω. For a wide range of i, a rough rule of thumb (18) is that pulses are single if $\omega_H/\omega \lesssim 10$, triple if $10 \lesssim \omega_H/\omega \lesssim 50$ and double if $\omega_H/\omega \gtrsim 50$. One should point out that Her X-1 and 4U0115+63, where ω_H is known, have L > few 10^{37} erg s^{-1}, which probably leads to radiative shocks from which mostly fan beams are expected. Observations of such correlations or their absence could help settle the fan-pencil and shock-Coulomb controversy.

Acknowledgements: It is a pleasure to thank E. Boldt, R. Ramaty, J. Swank, B. Teegarden and N. White for discussions.

References

1. Lewin, W. H., 1981, this volume.
2. Pringle, J., Rees, M. J., 1972, Astron. Astrophys 21, 1.
3. Davidson, K., Ostriker, J. P., 1973, Ap. J. 179, 585.
4. Lamb, F. K., Pethick, C., Pines, D., 1973, Ap. J., 184, 271.
5. Rappaport, S., Joss, P. C., 1980, M.I.T. prepr. CSR-HEA-80-24.

6. Rappaport, S., Joss, P. C., 1977, Nature, 266, 683.
7. Ghosh, P., Lamb, F. K., 1979, Ap. J., 234, 296.
8. Börner, G., 1980, Phys. Reports 60, 151.
9. Lamb, F.K., 1980, Proc. S.Chapman Conf., Battrick, Ed., E.S.A.
10. Gursky, H., Schreier, E., 1975, I.A.U. Symp. 67, Reidel.
11. Kolykhalov,P.I., Sunyaev,R.A., 1979, Sov. A. J. Lett. 5, 180.
12. Ramaty, R., et al., 1980, Nature 287, 122.
13. Terrell, J. et al., 1980, Nature 285, 383.
14. Shulman, S., et al., 1975, Ap. J., 199, L101.
15. Basko, M. M., Sunyaev, R. A., 1976, M.N.R.A.S. 175, 395.
16. McCray, R., Lamb, F. K., 1976, Ap. J. 204, L115.
17. Basko, M. M., Sunyaev, R. A., 1976, Sov. A. J. 20, 537.
18. Mészáros, P., Bonazzola, S., 1981, Ap. J. (in press).
19. Nagel, W., 1981a, Ap. J. (in press).
20. Pravdo, S., et al., 1977, Ap. J. 216, L23.
21. Boldt, E. A., et al., 1976, Astron. Astrophys. 50, 161.
22. Becker, R. H. et al., 1977, Ap. J. 214, 879.
23. Becker, R. H., et al., 1979, Ap. J. 227, L21.
24. White, N. E., et al., 1980, Ap. J. 239, 665.
25. White, N. E. and Pravdo, R. H., 1979, Ap. J. 233, L21.
26. Becker, R. H., et al., 1978, Ap. J. 221, 912.
27. Ross, R., Weaver, R., McCray, R., 1978, Ap. J. 219, 297.
28. Basko, M. M., 1980, Astron. Astrophys. 87, 330.
29. Nagel, W., 1980, Ap. J., 236, 904.
30. Mészáros, P., Nagel, W., Ventura, J., 1980, Ap. J., 238, 1066.
31. Yahel, R. Z., 1979, Ap. J. 229, L73.
32. Yahel, R. Z., 1980, Ap. J., 236, 911.
33. Pravdo, S. H. Bussard, R. W., 1981, Ap. J. Lett (in press).
34. Bonazzola, S., et. al. 1979, Astron, Astrophys. 78, 53.
35. Nagel, W., 1981b, Ap. J. (in press).
36. Bahcall, J., 1978, Ann. Rev. Astron. Astrophys. 16, 241.
37. Teegarden, B., Cline, T., 1980, Ap. J. 236, L67.
38. Mazets, E. P., et al., 1981, Nature, 282, 587.
39. Mazets, E. P., Golenetskii, S. V., 1981, Ap. Sp. Sci. 75, 47.
40. Ramaty, R., Mészáros, P., 1981, Ap. J., (in press).
41. Zdziarski, A. A., 1981, Acta Astronomica 30, 371.
42. Trümper, J., et al., 1977, Ann. New York Ac. Sci. 302, 538.

43. Trümper, J. et al., 1978, Ap. J. 219, L105.
44. Durouchoux, P., et al., 1978, Proc. NASA/GSFC Symp. Gamma Ray Spectroscopy, TM 79619.
45. Gruber, D. E., et al., 1980, Ap. J. 240, L127.
46. Tueller, J. et al., 1981, Proc. Int. Cosmic Ray Conf, Paris.
47. Wheaton, W. A., et al., 1979, Nature 282, 240.
48. Zeldovich, Ya. B., Shakura, N. I., 1969, Sov. A. J. 13, 175.
49. Alme, M. L., Wilson, J. R., 1973, Ap. J., 186, 1015.
50. Shapiro, S. L., Salpeter, E. E., 1975, Ap. J. 198, 671.
51. Gnedin, Yu.N., Sunyaev, R.A., 1979, Astr. Astrophys. 36, 379.
52. Basko, M.M., Sunyaev, R.A., 1975, Astron. Astrophys. 42, 311.
53. Daugherty, J. K., Ventura, J., 1977, Astr. Astrophys. 61, 723.
54. Mészáros, P., 1978, Astron. Astrophys. 63, L119.
55. Bussard, R. W., 1978, Proc. GSFC Symp. Gamma Ray Spectroscopy.
56. Weaver, R. P., 1978, Proc. GSFC Symp. Gamma Ray Spectroscopy.
57. Canuto, V., et. al., 1971, Phys. Rev. D, 3, 2303.
58. Daugherty, J. K., Ventura, J., Phys. Rev. D, 18, 1053.
59. Börner, G, Mészáros, P., 1979, 21, 357.
60. Ventura, J., 1979, Phys. Rev. D, 19, 1684.
61. Herold, H., 1979, Phys. Rev D, 19, 2868.
62. Novick, R., et al., 1977, Ap. J., 215, L117.
63. Mészáros, P., Ventura, J., 1978, Phys. Rev. Lett. 41, 1544.
64. Mészáros, P., Ventura, J., 1979, Phys. Rev. D, 19, 3565.
65. Gnedin, Yu. N., et. al., 1978, JETP (Lett) 27, 305.
66. Ventura, J., Nagel, W., Mészáros, P., 1979, Ap. J. 233, L125.
67. Pavlov, G. G., Shibanov, Yu. A., 1979, JETP 49, 741.
68. Virtamo, J., Jauho, P., 1975, Nuovo Cim. 16B, 537.
69. Kirk. J. G., Mészáros, P., 1980, Ap. J., 241, 1153.
70. Wasserman, I., Salpeter, E. E., 1980, Ap. J., 241, 1107.
71. Ventura, J., 1973, Phys. Rev. A., 8, 3021.
72. Basko, M. M., Sunyaev, R. A., 1975, JETP 41, 52.
73. Pavlov, G. G., Yakovlev, Yu. A., 1976, JETP 43, 389.
74. Kirk, J. G., 1979, Plasma Phys. 21, 1021.
75. Bussard, R. W., 1980, Ap. J., 237, 970.
76. Langer, S. H., 1981, Phys. Rev. D 23, 328.
77. Kirk, J. R., Galloway, J. J., 1981, M.N.R.A.S. 195, 45P.
78. Kirk, J.G., Galloway, D.J., 1981, M.P.I.-PAE/Astro 266 prepr.

79. Langer, S. H., McCray, R, Baan, W. A., 1980, Ap. J. 238, 731.
80. Yahel, R. Z., 1980, Astron.. Astrophys. 90, 26.
81. Kanno, S., 1980, Pub. Astr. Soc., Japan 32, 105.
82. Silant'ev, N. A., 1981, Ioffe Inst. (Leningrad) preprint 685.
83. Kaminker, A.D., et al., 1981, Ioffe Inst. (Leningrad) pr. 716.
84. AXAF Report, 1980, NASA/Marshall S. F. C., TM-78285.
85. Basko, M. M., Sunyaev, R. A., 1976, M.N.R.A.S. 175, 395.
86. Bonazzola, S., et al., 1981, Astron. Astrophys (in press).
87. Wang, Y. M., Frank, J., 1981, Astron. Astrophys (in press).

FIGURE CAPTIONS

Figure 1. Relation between period decrement P and $PL^{3/7}$, P being period, L the X-ray luminosity, for 9 X-ray pulsars, superimposed on theoretical curves based on disk accretion models (from Ref (7)).

Figure 2. Pulse shapes and periods for a number of X-ray pulsars (from Ref. (5)).

Figure 3. The X-ray spectrum of Her X-1, including the feature around 50 keV interpreted as due to the cyclotron effect in a field of 4.4×10^{12} Gauss (from Ref. (43)).

Figure 4. Neutron star mass limits derived from data on 5 X-ray pulsars and the binary radio pulsar. The shaded area indicates the range of values predicted by conventional equations of state (from Ref. (5)).

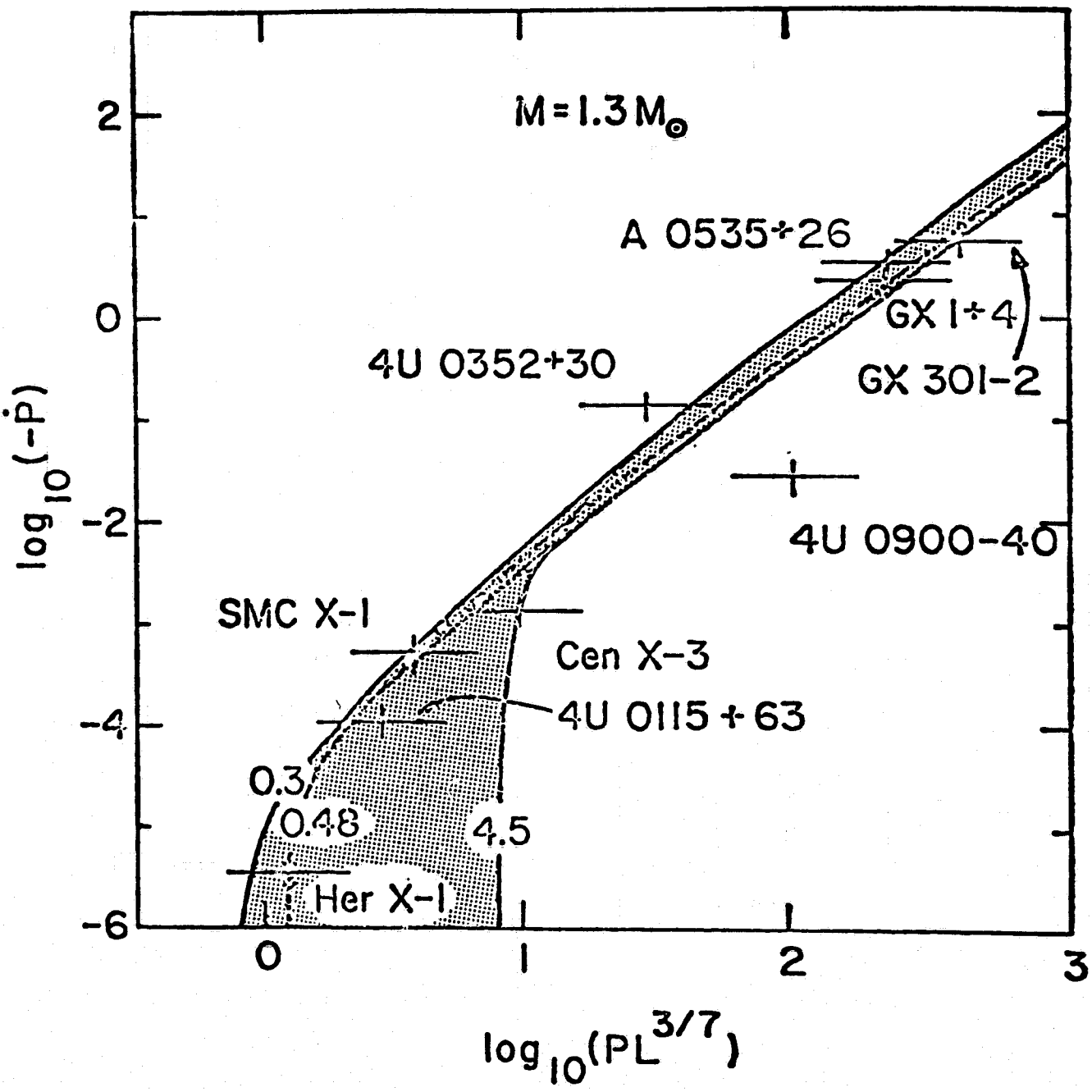
M=1.3 M⊙
A 0535+26
GX 1+4
GX 301-2
4U 0352+30
4U 0900-40
SMC X-1
Cen X-3
4U 0115+63
0.3
0.48
4.5
Her X-1
2
0
-2
-4
-6
0
1
2
3
log10(-Ṗ)
log10(PL3/7)

Fig.1

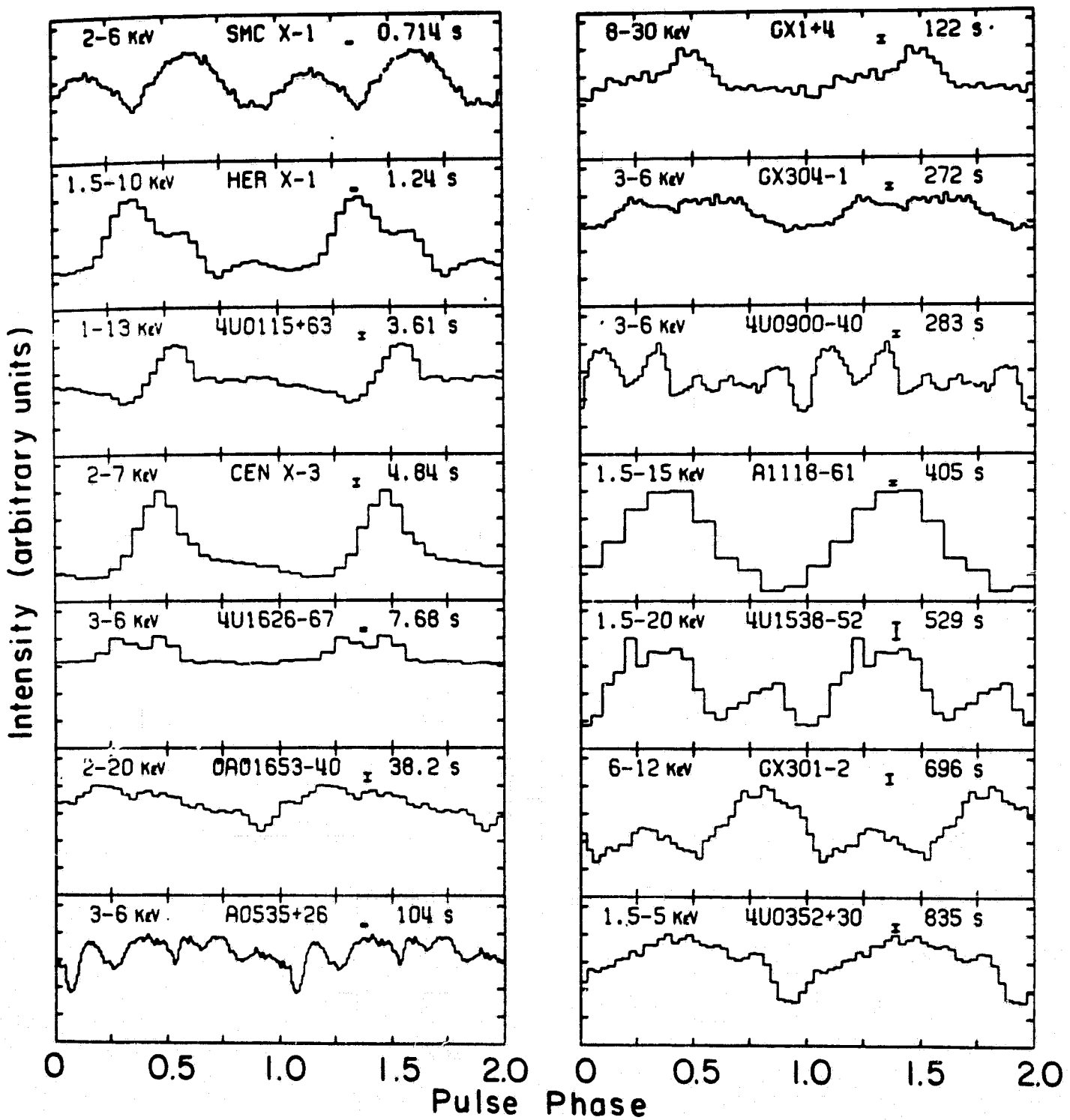
2-6 Kev
SMC X-1
0.714 s
1.5-10 Kev
HER X-1
1.24 s
1-13 Kev
4U0115+63
3.61 s
2-7 Kev
CEN X-3
4.84 s
3-6 Kev
4U1626-67
7.68 s
2-20 Kev
OAO1653-40
38.2 s
3-6 Kev
A0535+26
104 s
8-30 Kev
GX1+4
122 s
3-6 Kev
GX304-1
272 s
3-6 Kev
4U0900-40
283 s
1.5-15 Kev
A1118-61
405 s
1.5-20 Kev
4U1538-52
529 s
6-12 Kev
GX301-2
696 s
1.5-5 Kev
4U0352+30
835 s
Intensity (arbitrary units)
0
0.5
1.0
1.5
2.0
Pulse Phase

Fig.2

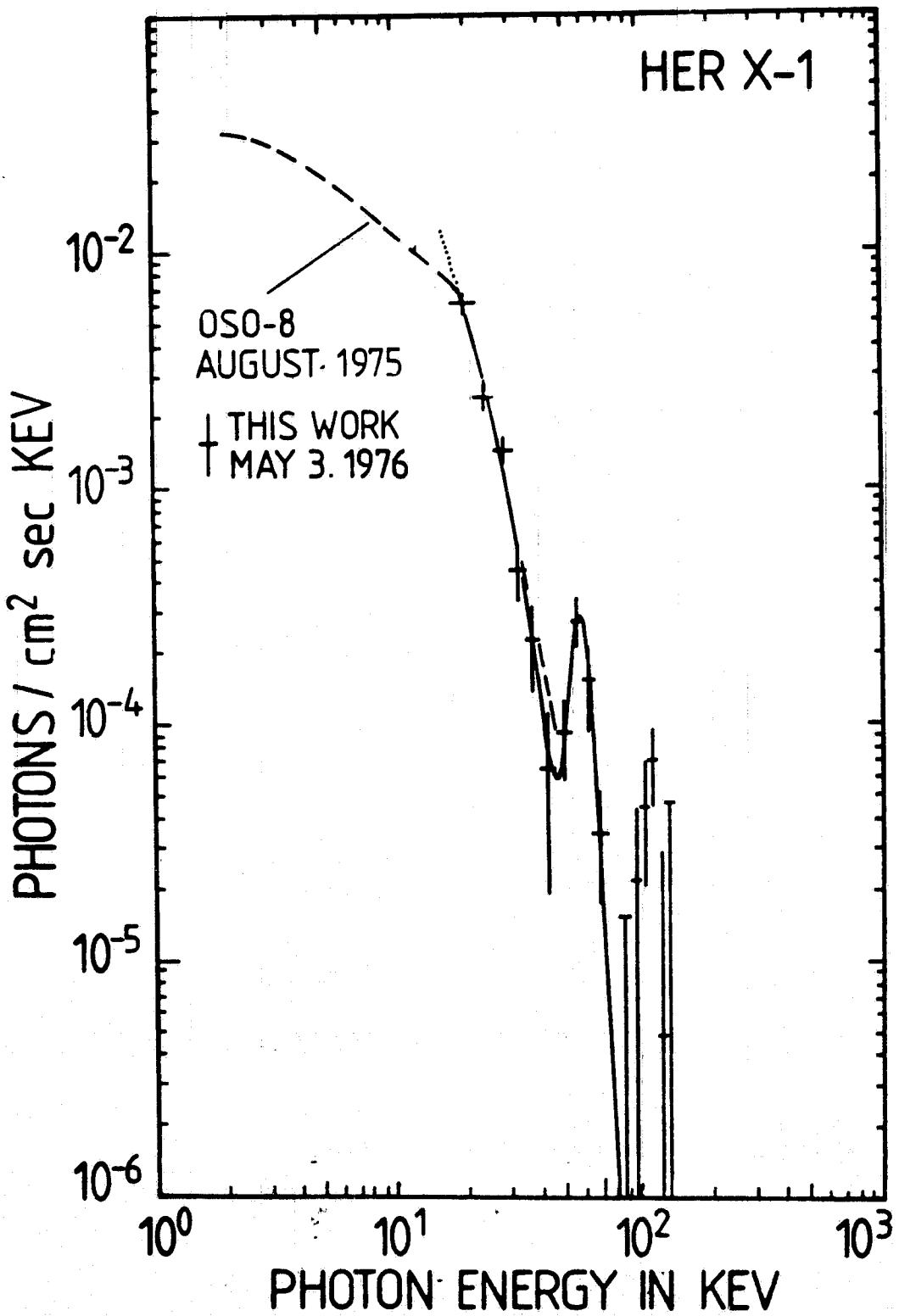
HER X-1
OSO-8
AUGUST 1975
THIS WORK
MAY 3. 1976
PHOTONS / cm² sec KEV
PHOTON ENERGY IN KEV
10⁻²
10⁻³
10⁻⁴
10⁻⁵
10⁻⁶
10⁰
10¹
10²
10³

Fig.3

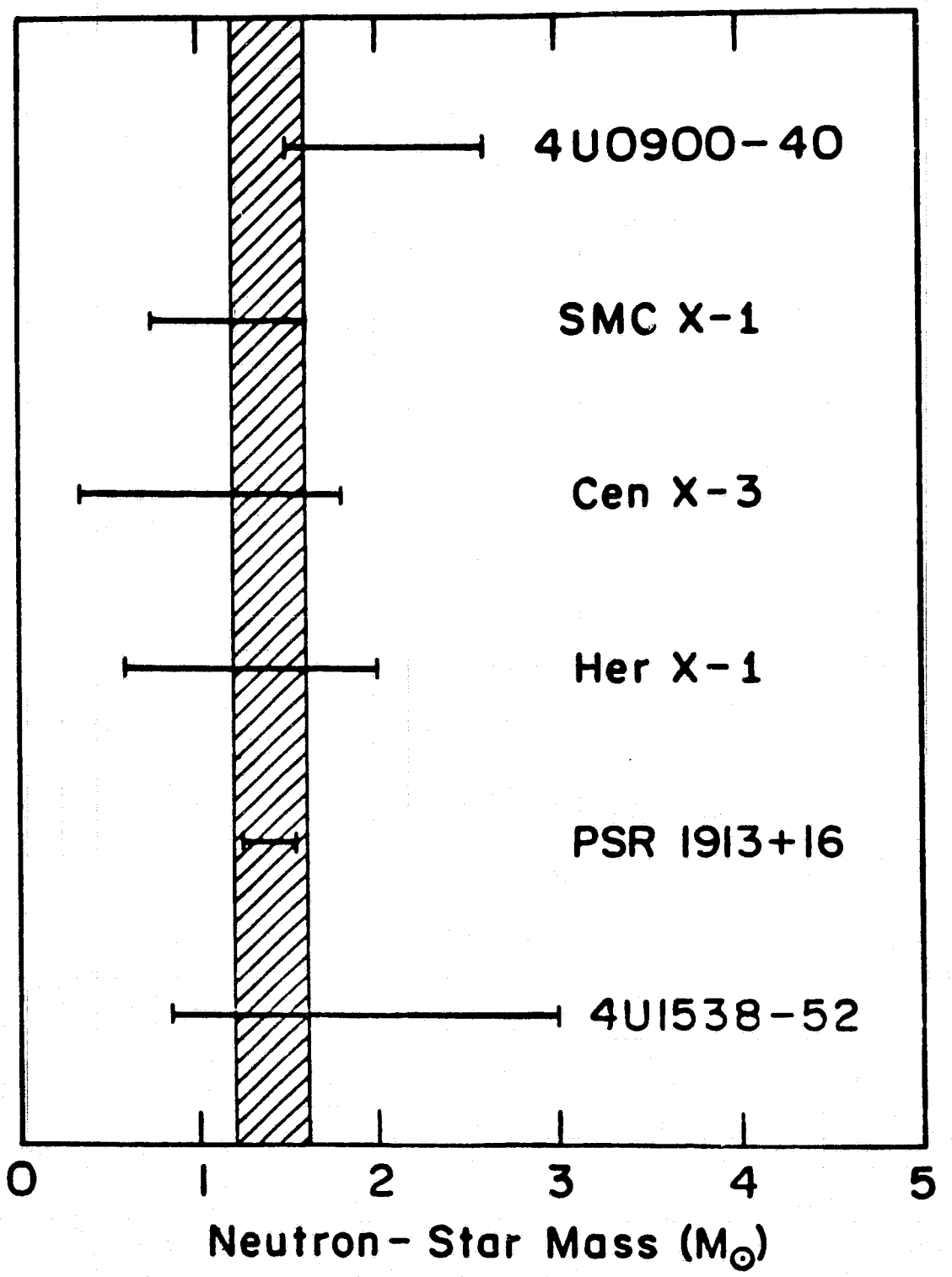
4U0900-40
SMC X-1
Cen X-3
Her X-1
PSR 1913+16
4U1538-52
0
1
2
3
4
5
Neutron-Star Mass ($M_\odot$)

Fig.4